JACS
JOURNAL OF THE AMERICAN CHEMICAL SOCIETY
Article
pubs.acs.org/JACS

Stereochemical Inversion of a Cyano-Stabilized Grignard Reagent: Remarkable Effects of the Ethereal Solvent Structure and Concentration

Ming Gao, Neeraj N. Patwardhan, and Paul R. Carlier*

Department of Chemistry, Virginia Tech, Blacksburg, Virginia 24061, United States

Supporting Information

ABSTRACT: Chiral organometallic reagents are useful in asymmetric synthesis, and configurational stability of these species is critical to success. In this study we followed the epimerization of a chiral Grignard reagent, prepared by Mg/Br exchange of bromonitrile *trans*-**2b**. This compound underwent highly retentive Mg/Br exchange in Et_2O; less retention was observed in 2-MeTHF and THF. Epimerization rate constants k_{tc} were determined at 195 K by measuring the diastereomer ratio of deuteration product d_1-**3b** as a function of the delay time before quench. Studies were also performed at varying concentrations of Et_2O in toluene. Remarkable dynamic range in k_{tc} was seen: relative to reaction at 0.12 M Et_2O in toluene, epimerization was 26-, 800-, and 1300-fold faster in Et_2O, 2-MeTHF, and THF, respectively. Thus, the identity and concentration of an ethereal solvent can dramatically affect configurational stability. Reaction stoichiometry experiments suggested that, in Et_2O, the Grignard reagent derived from *trans*-**2b** exists as an *i*-PrMgCl heterodimer; the invariance of k_{tc} over a 20-fold range in $[Mg]_{total}$ ruled out mandatory deaggregation (or aggregation) on the epimerization path. Analysis of the dependency of k_{tc} on $[Et_2O]$ and temperature in Et_2O/toluene solution at 195, 212, and 231 K indicated fast incremental solvation before rate-limiting ion-pair separation and provided an estimate of the entropic cost of capturing a solvent ligand (−13 ± 3 eu). Calculations at the MP2/6-31G*(PCM)//B3LYP/6-31G* level provide support for these conclusions and map out a possible "ionogenic conducted tour" pathway for epimerization.

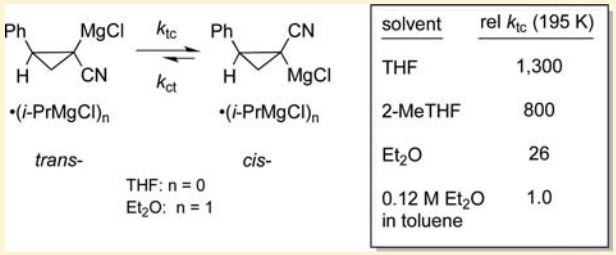

INTRODUCTION

Enantiomerically enriched organolithiums are valuable reagents in asymmetric synthesis.[1−7] To date enantiomerically enriched Grignard reagents have enjoyed less widespread use, although recent advances in the preparation of these reagents[8−15] should begin to reverse this deficit. Our efforts in this area have focused on enantioenriched cyclopropylnitrile Grignard reagent (*S*)-**1a**, which was first described by Walborsky, albeit in low enantiomeric purity.[16] We showed that (*S*)-**1a** could be prepared in high enantiomeric purity by Mg/Br exchange[17,18] of (*S*)-**2a** with *i*-PrMgCl and that it exhibited macroscopic configurational stability.[19] Though enantioenriched Grignard reagent (*S*)-**1a** was unreactive with carbon electrophiles below 0 °C, it underwent retentive deuteration. It thus provided an excellent platform from which to study the stereochemical fidelity of Mg/Br exchange and the rate of Grignard racemization. By monitoring the enantiomer ratios (er's) of the deuteration product d_1-**3a**,[20] we demonstrated that Mg/Br exchange of enantiopure bromide (*S*)-**2a** with *i*-PrMgCl was more highly retentive in Et_2O than in 2-methyltetrahydrofuran (2-MeTHF) or THF. In addition, the enantiomerization rate constant (k_{enant}) of (*S*)-**1a** was much smaller in Et_2O than in the other solvents (Scheme 1).[21]

Reaction stoichiometry studies suggested that Mg/Br exchange of (*S*)-**2a** with 2 equiv of *i*-PrMgCl in Et_2O gave rise to a heterodimer of (*S*)-**1a** with *i*-PrMgCl. Invariance of k_{enant} over a 25-fold range in $[Mg]_{total}$ indicated no change in aggregation state on the enantiomerization path; measurement of k_{enant} in ether/toluene solvent mixtures at 212 K showed a saturating dependence on $[Et_2O]$. Finally, Eyring analysis[22] of k_{enant} over the range 175−231 K revealed an unusually large negative entropy of activation for enantiomerization (−49 ± 4 eu). Together these observations pointed toward the racemization mechanism outlined in Scheme 2.

At low $[Et_2O]$, the resting state of the heterodimer was proposed to be the disolvate. Fast incremental solvation of the disolvated Grignard heterodimer (k_1/k_{-1}) precedes a slow stereochemical inversion (k_2). The negative entropy of activation for enantiomerization of the heterodimer observed in Et_2O was attributed to rate-limiting ion-pair separation, which would cause ordering of the secondary solvent shell (electrostriction).[23] Several previous studies on the enantiomerization of organolithiums[4,23−25] reported similarly large negative entropies of activation and had invoked either rate-limiting solvent capture or electrostriction. However, ours was the first study to conclusively demonstrate that incremental solvation preceded the rate-limiting enantiomerization step.

Received: July 17, 2013
Published: August 26, 2013

   dx.doi.org/10.1021/ja407348s | J. Am. Chem. Soc. 2013, 135, 14390−14400

Scheme 1. Generation, Enantiomerization, and Quenching of Cyclopropylnitrile Grignard Reagent (*S*)-1a in Et_2O, 2-MeTHF, and THF[a]

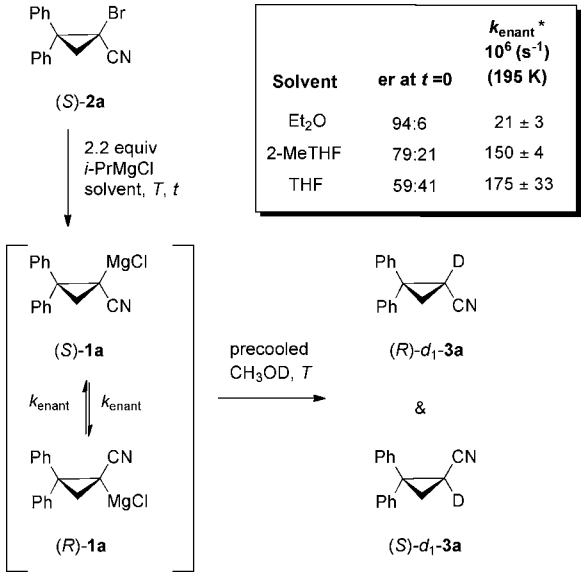

Solvent	er at t =0	k_{enant}* 10^6 (s^{-1}) (195 K)
Et_2O	94:6	21 ± 3
2-MeTHF	79:21	150 ± 4
THF	59:41	175 ± 33

[a]Note that **1a** is depicted as a monomer for simplicity only (vide infra).

Scheme 2. Proposed Mechanism for Enantiomerization of the 1a•*i*-PrMgCl Heterodimer in Et_2O and Epimerization of Related Grignard Reagent *trans*-1b[a]

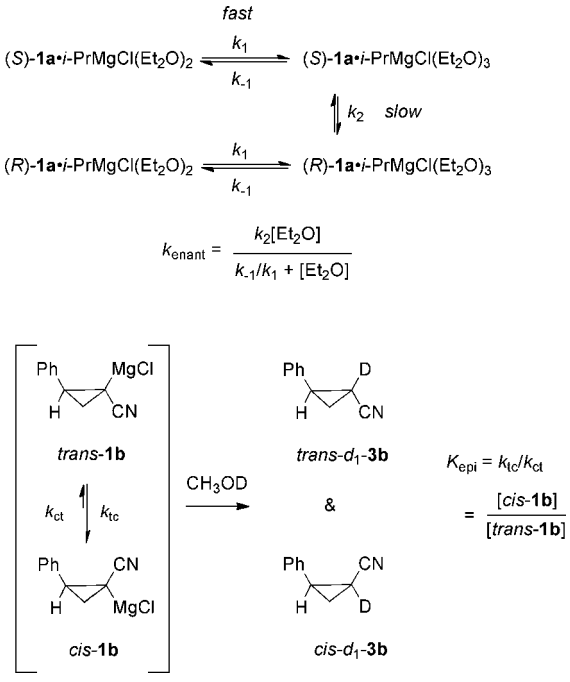

[a]Note: *trans* and *cis* designations of the Grignard reagent **1b** correspond to those of the CH_3OD quenching products *trans*- and *cis*-d_1-**3b**.

Since configurational stability is a key determinant of the synthetic utility of enantioenriched Grignard reagents, we believe that greater understanding of possible racemization mechanisms could serve to improve the stereochemical outcome of their reactions. Recent successes in the enantioselective trapping of configurationally stable lithiated[26] and magnesiated[15] nitriles also highlight the relevance of studying metalated nitriles such as (*S*)-**1a**. We were thus motivated to study stereochemical inversion of the analogous chiral Grignard reagent *trans*-**1b** (Scheme 2). This process is an epimerization, rather than a racemization, a distinction that presents both challenges and advantages. In the first part of this paper we will demonstrate remarkable solvent effects on the rate constant for epimerization of *trans*-**1b** (k_{tc}). These dramatic differences in configurational stability of a chiral Grignard reagent in closely related ethereal solvents should be of particular interest to those engaged in asymmetric synthesis. In the second part of this paper we describe further kinetic and reaction stoichiometry studies of *trans*-**1b**. The mechanism for epimerization of **1b** in Et_2O that emerges is consistent with our earlier studies on **1a**, but this work affords greater detail on the thermodynamics of solvation. This section concludes with computational studies that largely support our interpretation of kinetic data, including location of a transition structure for an "ionogenic conducted tour" mechanism for epimerization.

RESULTS AND DISCUSSION

Configurational Stability of *trans*-1b and Synthesis of Bromonitrile Precursors. To study the epimerization of *trans*-**1b**, it was necessary to first prepare suitable precursors. Although both Mg/Br[17,18] and Mg/sulfoxide[27,28] exchange routes to magnesiated nitriles are known, for continuity with our previous studies on **1a** (and to avoid the stereochemical complexity presented by the stereogenic sulfoxide S atom), we chose the former route. We thus prepared the corresponding bromonitriles *trans*- and *cis*-**2b** (Scheme 3).

Because we planned to use ^1H NMR spectroscopy to follow the extent of epimerization, *trans*- and *cis*-**2b** were prepared in racemic form. This decision was motivated by synthetic

Scheme 3. Synthesis of Bromonitrile Substrates *trans*- and *cis*-2b[a]

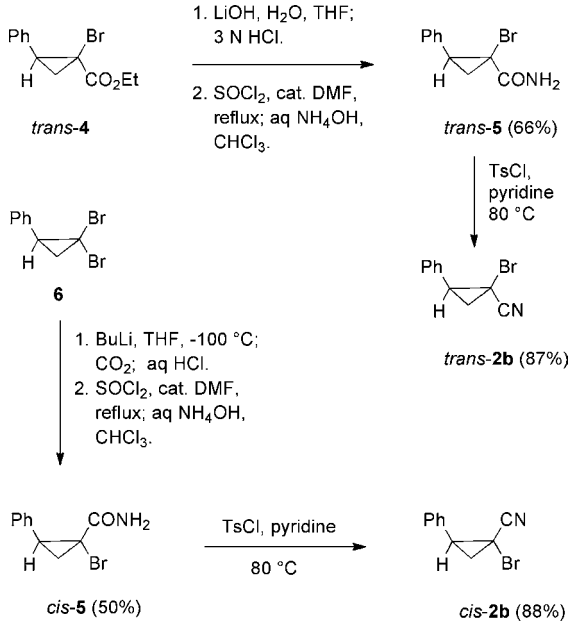

[a]Note that stereochemical descriptors are chosen to match those of the retentive Mg/Br exchange/deuteration products (*trans*- and *cis*-d_1-**3b**; see Scheme 2).

dx.doi.org/10.1021/ja407348s | J. Am. Chem. Soc. 2013, 135, 14390−14400

expedience and by the expectation that the racemic nature of the Grignard reagents would not complicate the kinetic analysis of epimerization. Our results below will justify that assumption. Synthesis of *trans*-**2b** began with bromocyclopropane carboxylic ester *trans*-**4**, which was prepared in 83% yield using Hansen's two-step protocol.[29] Standard transformation to the primary amide *trans*-**5**, followed by dehydration.[19] yielded the desired bromonitrile *trans*-**2b**. Synthesis of the *cis*-isomer began with the known 1,1-dibromocyclopropane **6**.[30] Stereoselective Mg/Br exchange and treatment with CO_2 gave the carboxylic acid,[31] which was converted directly to primary amide *cis*-**5** (50% yield after two steps). Dehydration then gave the desired bromonitrile *cis*-**2b**.

Unlike Grignard reagent **1a**, which at equilibrium exists as an equal mixture of enantiomers, **1b** will exist at equilibrium as an unequal mixture of *trans*- and *cis*-diastereomers (Scheme 2). As will be shown below, to determine the epimerization rate constant k_{tc} (tc designates *trans* to *cis*), it is necessary to know the epimerization equilibrium constant K_{epi}, defined as k_{tc}/k_{ct}, or [*cis*-**1b**]/[*trans*-**1b**]. To determine K_{epi}, we sought conditions under which Mg/Br exchange−deuteration of *trans*- and *cis*-**2b** gave identical diastereomer ratios (dr's) for the deuteration products d_1-**3b**. Since (*S*)-**1a** was demonstrated to show retentive protonation/deuteration (as high as 98:2 er),[21] we presumed that *trans*- and *cis*-**2b** (and corresponding *i*-PrMgCl heterodimers) would also undergo retentive protonation/deuteration. Thus, the dr of the deuteration products d_1-**3b** would provide a measure of the dr of the corresponding Grignard reagents. Because the approach to equilibrium was very slow at 195 K, we carried out the experiments at 273 and 231 K (Table 1).

Table 1. Determination of K_{epi} for Epimerization of *trans*-1b at 273 and 231 K[a]

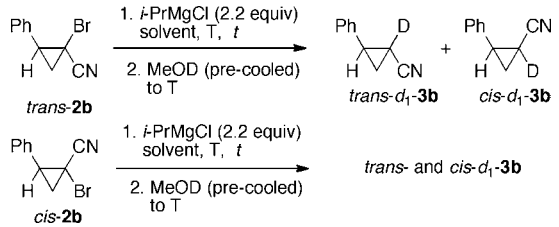

entry	solvent	T (K)	K_{epi}[b]	calcd ΔG_{epi} (kcal/mol)
1	Et_2O	273	4.4 ± 0.6	−0.80 ± 0.06
2		231	5.8 ± 0.8	−0.80 ± 0.06
3	2-MeTHF	273	13 ± 2	−1.38 ± 0.06
4		231	19 ± 3	−1.36 ± 0.06
5	THF	273	19 ± 3	−1.59 ± 0.06
6		231	28 ± 4	−1.58 ± 0.06

[a]Reactions performed at $[Mg]_{total}$ = 0.110 M. [b]K_{epi} is defined in Scheme 2 and is calculated from the dr of d_1-**3b** as determined by ^{1}H NMR integration; separate reactions of *trans*- and *cis*-**2b** gave identical dr's within experimental error. The error in each NMR integration was assumed to be ±10%, and the errors in K_{epi} and ΔG_{epi} were then calculated according to standard propagation of error.[32]

As shown in the Supporting Information, excellent ^{1}H NMR spectroscopic resolution of *cis*- and *trans*-d_1-**3b** enabled reliable dr determination. Furthermore, the ^{1}H NMR signals of *cis*- and *trans*-d_1-**3b**, their protio analogues **3b**, and the corresponding bromonitriles **2b** were all well separated. In this way ^{1}H NMR spectroscopy in each case confirmed >98% conversion of *cis*- or *trans*-**2b** and >98% deuterium incorporation in **3b**. This latter observation indicated that the Grignard reagent resulting from Mg/Br exchange did not induce elimination of the *i*-PrBr coproduct. At 273 K in Et_2O, equilibrium was reached within 5 min, as demonstrated by the identical dr's (within error) obtained from reaction of *trans*- and *cis*-**2b** (Supporting Information). Equilibration at 231 K was slower, and a 30 min delay before CH_3OD quench was required to achieve similar dr values from reaction of *trans*- and *cis*-**2b**. These data indicate that at equilibrium in Et_2O there is a modest preference for *cis*-**7b** (K_{epi} = 4.4−5.8). The associated Gibbs free energy (ΔG_{epi}) values at 273 and 231 K are identical within error (Table 1, entries 1 and 2). Thus, within error, ΔS_{epi} in Et_2O is 0 eu. In 2-MeTHF and THF, the same general phenomena were observed, although the preference for *cis*-**1b** is greater. Again the calculated ΔG_{epi} values at 273 and 231 K are identical within error, indicating $\Delta S_{epi} \approx 0$ eu. Thus, on the basis of the calculated ΔG_{epi} values, the magnitude of K_{epi} at any temperature can be calculated (Supporting Information). Overall, the energetic preference for the *cis*-Grignard reagent ranges from −0.8 to −1.6 kcal/mol (Et_2O and THF, respectively, Table 1); we believe the *trans* to *cis* epimerization is driven by relief of steric strain between the 2-phenyl substitutent and the solvated Mg atom (Scheme 2).

We then turned our focus to determining epimerization rate constants k_{tc} as a function of the temperature and solvent. Assuming epimerization to be a reversible first-order reaction, we applied the standard kinetic treatment[33] to arrive at the following equation (see the Supporting Information for derivation):

$$\ln\left[\frac{(1 + K_{epi})X_t - 1}{K_{epi}}\right] = -(1 + 1/K_{epi})k_{tc}t \quad (1)$$

Thus, k_{tc} can be determined from X_t, the mole fraction of *trans*-d_1-**3b**, as a function of the epimerization time t that elapses before addition of the CH_3OD quench. In this way we determined k_{tc} at 195 K in Et_2O, 2-MeTHF, and THF (Figure 1)

In Et_2O at 195 K the values of k_{tc} of *trans*-**1b** and k_{enant} of **1a** were quite similar (cf. Figure 1 and Scheme 1), indicating very similar free energies of activation for stereochemical inversion (15.5 ± 0.1 and 15.4 ± 0.1 kcal/mol, respectively).

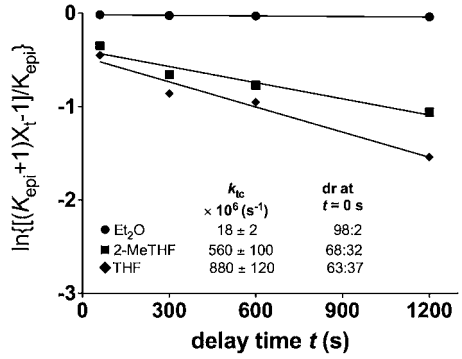

Figure 1. Determination of epimerization rate constants k_{tc} and extrapolated t = 0 dr for **1b**/*trans*-**7b** at 195 K and $[Mg]_{total}$ = 0.110 M in Et_2O, 2-MeTHF, and THF. The rate constants k_{tc} derive from the slopes $-(1 + 1/K_{epi})k_{tc}$ of each line; the extrapolated dr values at t = 0 are provided by X_t at t = 0, which can be calculated from the y-intercept of each line. The structure of *trans*-**7b** is given in Scheme 4.

dx.doi.org/10.1021/ja407348s | J. Am. Chem. Soc. 2013, 135, 14390−14400

Furthermore, as was seen for **1a**, the magnitude of the epimerization rate constants k_{tc} of *trans*-**1b** increased in the series Et_2O < 2-MeTHF < THF. However, whereas k_{enant} for **1a** was only 8-fold greater in THF than it was in Et_2O, k_{tc} for *trans*-**1b** was 49-fold greater in THF than it was in Et_2O. In addition, as was seen for (*S*)-**2a**, Mg/Br exchange of *trans*-**2b** was most retentive in Et_2O (the extrapolated t = 0 dr was 98:2), with significant loss of stereochemical purity in 2-MeTHF and THF. Thus, the choice of ethereal solvent can have dramatic consequences not only for configurational stability, but also for the stereochemical fidelity of Mg/Br exchange.

To further probe the effect of the solvent on configurational stability, we determined k_{tc} in Et_2O/toluene mixtures at 195, 212, and 231 K (Table 2). At 195 K, the epimerization rate constant k_{tc} at 0.12 M Et_2O in toluene was 20-fold smaller than it was in pure Et_2O. Similar but smaller decreases in k_{tc} with decreasing $[Et_2O]$ were also seen at 212 and 231 K. Overall, at 195 K remarkable dynamic range in k_{tc} was seen: relative to reaction at 0.12 M Et_2O in toluene, epimerization was 26-, 800-, and 1,300-fold faster in Et_2O, 2-MeTHF, and THF, respectively (cf. Figure 1). These results clearly show that both the identity and the concentration of an ethereal solvent can dramatically affect the configurational stability of a chiral organometallic.

Table 2. Values of k_{tc} as a Function of $[Et_2O]$ at 195, 212, and 231 K[a]

entry	T (K)	$[Et_2O]^b$ (M)	$10^6 k_{tc}$ (s^{-1})
1	195	9.5	14 ± 2
2	195	1.9	12 ± 2
3	195	0.48	9.4 ± 1.2
4	195	0.24	5.3 ± 0.5
5	195	0.12	0.70 ± 0.07
6	212	9.5	64 ± 7
7	212	1.9	49 ± 7
8	212	0.48	25 ± 23
9	212	0.24	21 ± 3
10	212	0.12	16 ± 3
11	231	9.5	1800 ± 200
12	231	1.9	1200 ± 200
13	231	0.48	550 ± 50
14	231	0.24	270 ± 50
15	231	0.12	120 ± 20

[a]Reactions performed with 2.2 equiv of *i*-PrMgCl at $[Mg]_{total}$ = 0.0125 M. [b]The concentration of neat Et_2O was taken as 9.5 M at 195, 212, and 231 K; other values represent concentrations of Et_2O in toluene based on densities at 25 °C.

Proposed Structure of *trans*-1b and Mechanism for Its Epimerization in Et_2O. The use of 2.2 equiv of *i*-PrMgCl in our Mg/Br exchange reactions of *trans*-**2b** deserves comment. In our previous study of Mg/Br exchange of **2a**,[21] we noted that the amount of *i*-PrMgCl needed for full conversion depended on the solvent. In THF, 1.1 equiv of this reagent gave full conversion of (±)-**2a**, as measured by ^{1}H NMR (Table 3, entry 1). Quantitation of the amount of *i*-PrBr was carried out by GC/MS, and 90 ± 4% of the expected amount of this coproduct was detected. However, in Et_2O, 1.1 equiv of *i*-PrMgCl did not give full conversion of (±)-**2a** nor full production of *i*-PrBr (Table 1, entry 2). Full conversion of (±)-**2a** (and full production of *i*-PrBr) was achieved with the use of 2.2 equiv of *i*-PrMgCl (Table 3, entry 3). In this work,

Table 3. Stoichiometry of Mg/Br Exchange Reactions of (±)-2a and *trans*-2b with *n* equiv of *i*-PrMgCl in Et_2O and THF at 212 K

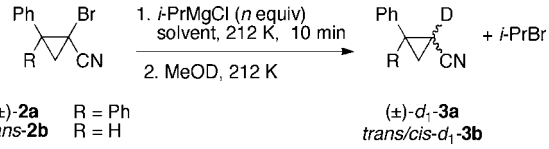

(±)-**2a** R = Ph
trans-**2b** R = H

(±)-d_1-**3a**
trans/cis-d_1-**3b**

entry	substrate	solvent	n	conversion of (±)-2a/*trans*-2b[a] (%)	concn of *i*-PrBr produced[b] (mol %)
1	(±)-**2a**	THF	1.1	>98[c]	90 ± 4[c]
2		Et_2O	1.1	59 ± 4[c]	65 ± 4[c]
3		Et_2O	2.2	>98[c]	92 ± 4[c]
4	*trans*-**2b**	THF	1.1	>98	91 ± 4
5		Et_2O	1.1	55 ± 4	59 ± 4
6		Et_2O	2.2	>98	95 ± 4

[a]Determined from ^{1}H NMR spectroscopy integrations, measuring the mole fraction of remaining reactants relative to products. All solutions of *i*-PrMgCl were titrated[34] prior to use. [b]Determined by GC/MS using mesitylene as an internal standard. [c]Data reported previously.[21]

the same experiments were repeated with *trans*-**2b** (Table 3, entries 4–6).

Reaction of *trans*-**2b** with 1.1 equiv of *i*-PrMgCl in THF at 212 K for 10 min, followed by MeOD quench, gave >98% conversion of *trans*-**2b** and 91 ± 4% of the expected amount of *i*-PrBr. However, just as was seen for (±)-**2a**, reaction of *trans*-**2b** with 1.1 equiv of *i*-PrMgCl in Et_2O gave only 55 ± 4% conversion and only 59 ± 4% of the expected amount of *i*-PrBr. When 2.2 equiv of *i*-PrMgCl was used, full conversion of *trans*-**2b** and full production of *i*-PrBr were observed. Together the reactions of (±)-**2a** and *trans*-**2b** with 1.1 equiv *i*-PrMgCl are consistent with the following scenario. In THF, alkylmagnesium chlorides (such as *i*-PrMgCl) are known to be predominantly monomeric.[35] Thus, Mg/Br exchange of (±)-**2a**/*trans*-**2b** with 1 equiv of *i*-PrMgCl occurs smoothly to give Grignard reagents **1a,b**, which are also presumably monomeric (Scheme 4, top). However, alkylmagnesium chlorides are known to be dimeric in Et_2O;[35–37] thus, 1 equiv of *i*-PrMgCl constitutes 0.5 equiv of the dimer. Reaction of 0.5 equiv of $[i\text{-PrMgCl}]_2$ with 1.0 equiv of (±)-**2a**/*trans*-**2b** could initially proceed to 0.5 equiv of the Grignard heterodimers **7a,b**. The results depicted in Table 1 can then be explained if (1) heterodimers **7a,b** is very sluggish toward further Mg/Br exchange with bromonitrile (±)-**2a**/*trans*-**2b** and (2) disproportionation of the heterodimers **7a,b** to magnesiated nitrile homodimers **8a,b** and $[i\text{-PrMgCl}]_2$ is also slow. Thus, in Et_2O, 2 equiv of *i*-PrMgCl (i.e., 1 equiv of $[i\text{-PrMgCl}]_2$) is needed to fully convert (±)-**2a** and *trans*-**2b** to the corresponding Grignard reagents.

Given the data that suggest that **2a** and *trans*-**2b** react with $[i\text{-PrMgCl}]_2$ in Et_2O to give heterodimers **7a** and **7b**, the possible involvement of deaggregation (or further aggregation) in the epimerization mechanism must be addressed. We thus examined whether the value of k_{tc} determined was affected by the total concentration of Mg species ($[Mg]_{total}$, Table 4). As can be seen, within error, at 212 K the value of k_{tc} did not change over a 20-fold change in $[Mg]_{total}$. Figure 1 and Table 2 also report values of k_{tc} in pure Et_2O at 195 K that are identical within error, even though they were measured at $[Mg]_{total}$ values differing by 9-fold (0.110 and 0.0125 M). These data thus rule out required deaggregation or further aggregation on

dx.doi.org/10.1021/ja407348s | J. Am. Chem. Soc. 2013, 135, 14390–14400

Scheme 4. Proposed Course for Mg/Br Exchange of (±)-2a/*trans*-2b with 1 equiv of *i*-PrMgCl in THF and Et_2O[a]

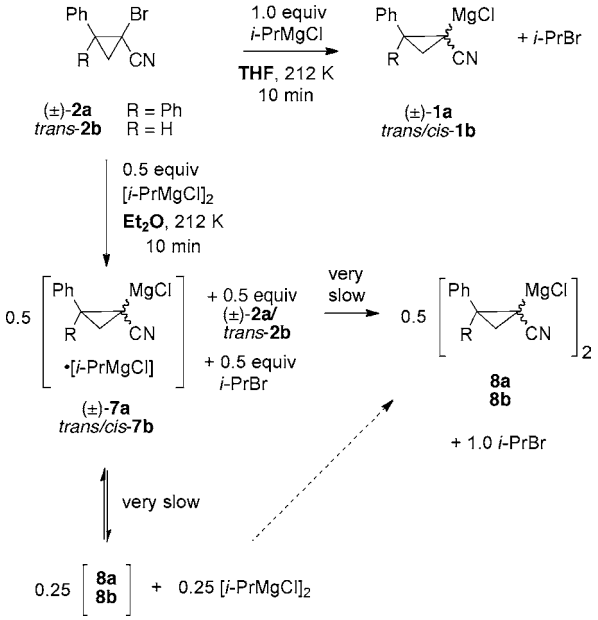

[a]Associated solvent ligands are omitted for simplicity; if formed, **8a** and **8b** would comprise a mixture of stereoisomers.

Table 4. Values of k_{tc} as a Function of $[Mg]_{total}$ at 212 K in Et_2O

entry	$[Mg]_{total}$ (M)	$10^6 k_{tc}$ (s^{-1})	entry	$[Mg]_{total}$ (M)	$10^6 k_{tc}$ (s^{-1})
1	0.125	86 ± 12	3	0.0125	64 ± 7
2	0.025	68 ± 8	4	0.00625	68 ± 8

the epimerization path and validate the first-order kinetic approach outlined in eq 1. Finally, the evidence ruling out the intermediacy of magnesiated nitrile homodimer **8b** or higher aggregates of **7b** justifies the use of racemic *trans*-**2b** in these studies.

As mentioned in the Introduction, k_{enant} of **7a** displayed a saturating dependence on $[Et_2O]$ at 212 K. The data for **7b** at 195, 212, and 231 K listed above in Table 2 cover an 80-fold range, from 9.5 M (neat Et_2O) to 0.12 M Et_2O in toluene, and were thus similarly analyzed (Figure 2). The k_{tc} data for epimerization of *trans*-**7b** were fitted to $[Et_2O]$ using a simple two-parameter (k_{-1}/k_1, k_2) saturation model, as we had done previously for enantiomerization of (*S*)-**7a**. The relationship of these parameters to k_{tc} and $[Et_2O]$ arises from the proposed mechanism (Scheme 5); the full derivation is given in the Supporting Information.

Following our conclusions for the enantiomerization of **7a** (Schemes 2 and 4), we propose that the resting state of the heterodimer *trans*-**7b** at low $[Et_2O]$ (<2 M) is a disolvate. Such species would have a coordination number of 4 at each Mg atom, and the calculations described below support this proposal. As can be seen from Scheme 5, the measured term k_{-1}/k_1 is the inverse of the equilibrium constant K_{solv} for incremental solvation of the heterodimer disolvate to the trisolvate. If the kinetic model in Scheme 5 is correct, the temperature dependence of K_{solv} should reflect the entropic cost of coordinating one molecule of Et_2O. We thus transformed the measured values of k_{-1}/k_1 to K_{solv} and then

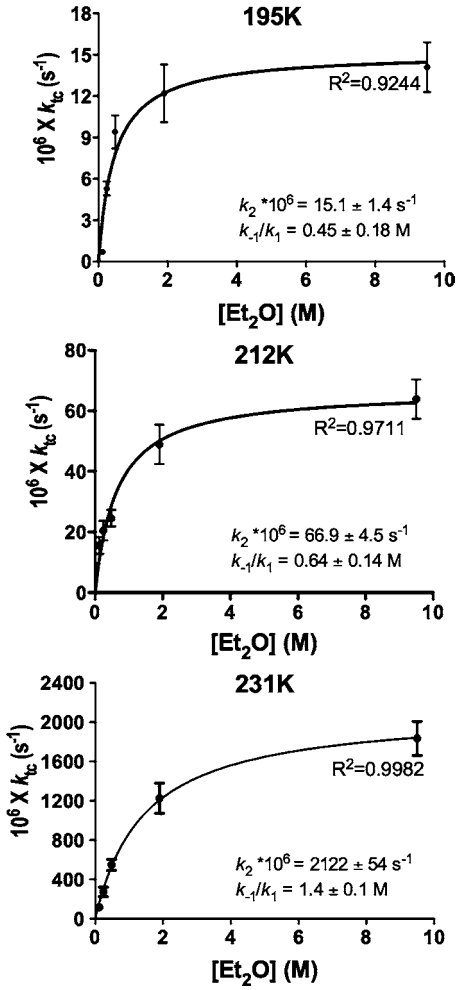

Figure 2. k_{tc} vs $[Et_2O]$ in toluene cosolvent at 195, 212, and 231 K and $[Mg]_{total}$ = 0.0125 M. Values of k_{tc} are taken from Table 2; see Scheme 5 for the definitions of k_2, k_{-1}, and k_1 and the equation relating them and $[Et_2O]$ to k_{tc}.

Scheme 5. Kinetic Scheme for the Epimerization of *trans*-7b, Relation of Epimerization Rate Constant k_{tc} to Microscopic Rate Constants, and Definition of K_{solv}

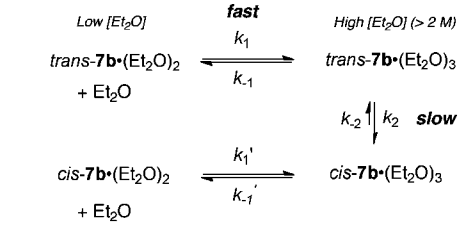

$$k_{tc} = \frac{k_2[Et_2O]}{k_{-1}/k_1 + [Et_2O]} \qquad K_{solv} = \frac{k_1}{k_{-1}} = \frac{[trans\text{-}\mathbf{7b}\bullet(Et_2O)_3]}{[trans\text{-}\mathbf{7b}\bullet(Et_2O)_2]\,[Et_2O]}$$

to the corresponding free energies ΔG_{solv} and plotted them versus temperature (Figure 3).

As shown in Figure 3, incremental solvation is nearly thermoneutral, with ΔG_{solv} ranging from −0.30 to +0.17 kcal/mol. Yet within error, ΔG_{solv} changes with temperature, and the extrapolated value of ΔS_{solv} is −13 ± 3 eu. This value appears consistent with the cost of associating an additional ether ligand. Finally, using values of k_{tc} in Table 2, Eyring analysis was

dx.doi.org/10.1021/ja407348s | J. Am. Chem. Soc. 2013, 135, 14390−14400

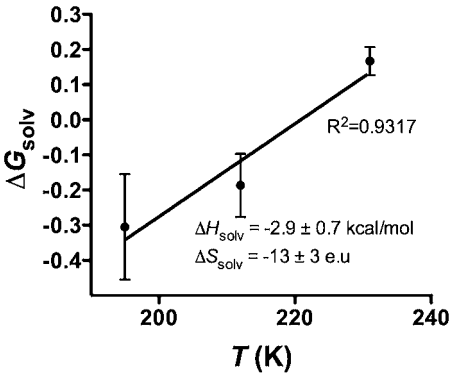

Figure 3. Temperature dependence of ΔG_{solv} (calculated from K_{solv}, Scheme 5).

performed at five different concentrations of Et_2O (Supporting Information). Enthalpies of activation for epimerization ($\Delta H^{\ddagger}_{epi}$) of *trans*-**7b** range from 9.3 ± 1.8 to 12.4 ± 1.4 kcal/mol, somewhat higher than our previous estimate of $\Delta H^{\ddagger}_{enant}$ for **7a** (5.7 ± 0.8 kcal/mol). Entropies of activation for epimerization ($\Delta S^{\ddagger}_{epi}$) range from −21 ± 13 to −34 ± 9 eu, still significantly negative but smaller than our previous estimate of $\Delta S^{\ddagger}_{enant}$ for **7a** (−49 ± 4 eu). Thus, like enantiomerization of **7a**, epimerization of *trans*-**7b** also appears to be accompanied by solvent electrostriction,[23] consistent with an ionogenic rate-determining step (such as ion-pair separation).

Given that the same kinetic behavior was seen for stereochemical inversion of Grignard heterodimers **7a** and *trans*-**7b**, we judged that it would be useful to undertake computational studies on the structure of the possible intermediates. These studies could provide insight into the atomic connectivity of the proposed heterodimers and their equilibrium solvation numbers. To model **7a,b**, we chose to study *i*-PrMgCl heterodimers of (1-cyanocyclopropyl)magnesium chloride (**1c**), which lacks the phenyl rings present in **1a** and **1b**. Two basic structural types for the heterodimers were considered: **9c**, which features a bis(μ-Cl) core and a η^1-(C)-cyclopropylnitrile unit, and **10c**, which features bridging chloride and cyclopropylnitrile nitrile moieties (Table 5).

The bis(μ-Cl) core embodied by **9c** has been seen by X-ray crystallography for cyclopentadienylmagnesium[38] and phosphavinylmagnesium[39] chloride etherates, and the bridging cyclopropylnitrile motif in **10c** has been demonstrated in the solid state by Boche for a lithiated cyclopropylnitrile.[40] Geometries for the solvent-free and bis- and tris(Et_2O) solvates were located at B3LYP/6-31G* and characterized as minima by vibrational frequency analysis. Higher solvates were explored, but no closed dimers with higher solvation numbers could be located. Occasionally these starting geometries led to open dimers (e.g., structures featuring a single bridging ligand),[41] but none of these structures were energetically competitive with solvates of the closed dimers **9c** and **10c**. Relative free energies (ΔG_{195}) of unsolvated and solvated **9c** and **10c** were calculated by a multistep process. First, PCM (Et_2O) single-point energies on the optimized geometries were calculated to model bulk solvent effects. Both the B3LYP and MP2 methods were employed, since several computational studies of organolithiums[42,43] and lithium amides[44] suggest that the MP2 method better estimates the energetic benefit of ethereal solvation. Second, free energy corrections to the electronic energies were obtained from the B3LYP/6-31G* frequencies, and correction to the standard state[45,46] was made to reflect

Table 5. Calculated Relative Free Energies of Unsolvated and Solvated Grignard Reagent Heterodimers in Pure Et_2O at 195 K

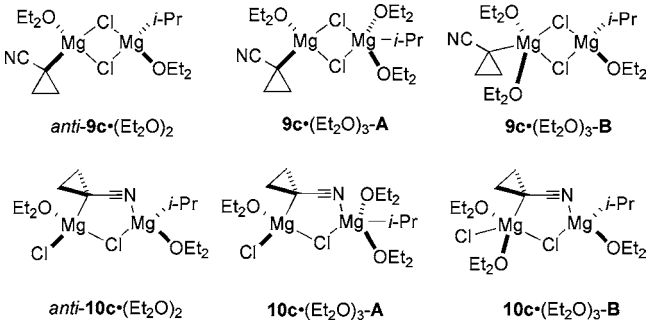

structure[a]	ΔG_{195} (kcal/mol) B3LYP/6-31G*(PCM)// B3LYP/6-31G*	ΔG_{195} (kcal/mol) MP2/6-31G* (PCM)// B3LYP/6-31G*
9c	13.5	23.2
anti-**9c**·$(Et_2O)_2$	7.6	3.9
syn-**9c**·$(Et_2O)_2$	6.5	3.4
9c·$(Et_2O)_3$-**A**	21.5	6.8
9c·$(Et_2O)_3$-**B**	15.0	1.6
10c	6.1	18.3
anti-**10c**·$(Et_2O)_2$	0.0	0.0
syn-**10c**·$(Et_2O)_2$	2.6	2.4
10c·$(Et_2O)_3$-**A**	11.8	1.8
10c·$(Et_2O)_3$-**B**	9.7	0.9
11c*·$(Et_2O)_3$	21.4	15.6
11c·$(Et_2O)_3$	19.6	15.3

[a]The *anti* and *syn* designations of the disolvates describe the relationship of the coordinated Et_2O ligands. The trisolvates (**A** and **B**) differ in the location of the third Et_2O ligand, as defined at the head of the table. The structures of **11c***·$(Et_2O)_3$ and **11c**·$(Et_2O)_3$ are given in Figure 4.

equilibria in pure Et_2O. Finally, to allow comparison of the free energies of the unsolvated and disolvated species with those of the trisolvates, those of the former species were adjusted by adding the free energies of three and one molecule(s) of Et_2O, respectively.

Looking at the relative free energies (ΔG_{195}) given in Table 5, the following conclusions can be drawn. First, at both the B3LYP and MP2 levels, the most stable species is the cyclopropylnitrile-bridged disolvate *anti*-**10c**·$(Et_2O)_2$. Second, the free energies of the other species relative to *anti*-**10c**·$(Et_2O)_2$ depend significantly upon the method chosen. We place greater stock in the ΔG_{195} values calculated from MP2/6-31G* PCM single-point energies, since (as mentioned previously) the MP2 method better estimates the energetic benefits of ethereal solvation. Focusing on these MP2-derived ΔG_{195} values, *anti*-**10c**·$(Et_2O)_2$ is 23.2 and 18.3 kcal/mol more stable than unsolvated **9c** and **10c**, respectively. Third, at the MP2 level, three trisolvates are within 2.0 kcal/mol of *anti*-**10c**·$(Et_2O)_2$, namely, **9c**·$(Et_2O)_3$-**B**, **10c**·$(Et_2O)_3$-**A**, and **10c**·$(Et_2O)_3$-**B**. The similarity in calculated ΔG_{195} values for these di- and trisolvates is thus consistent with our measured values of K_{solv}, which show that incremental solvation of the resting species at low [Et_2O] is nearly thermoneutral (Figure 3).

We then made an attempt to map out the beginning of a stereochemical inversion potential surface. Starting from the lowest energy trisolvate **10c**·$(Et_2O)_3$-**B**, we located ion-pair separation transition structure **11c***·$(Et_2O)_3$, as well as the

dx.doi.org/10.1021/ja407348s | J. Am. Chem. Soc. 2013, 135, 14390−14400

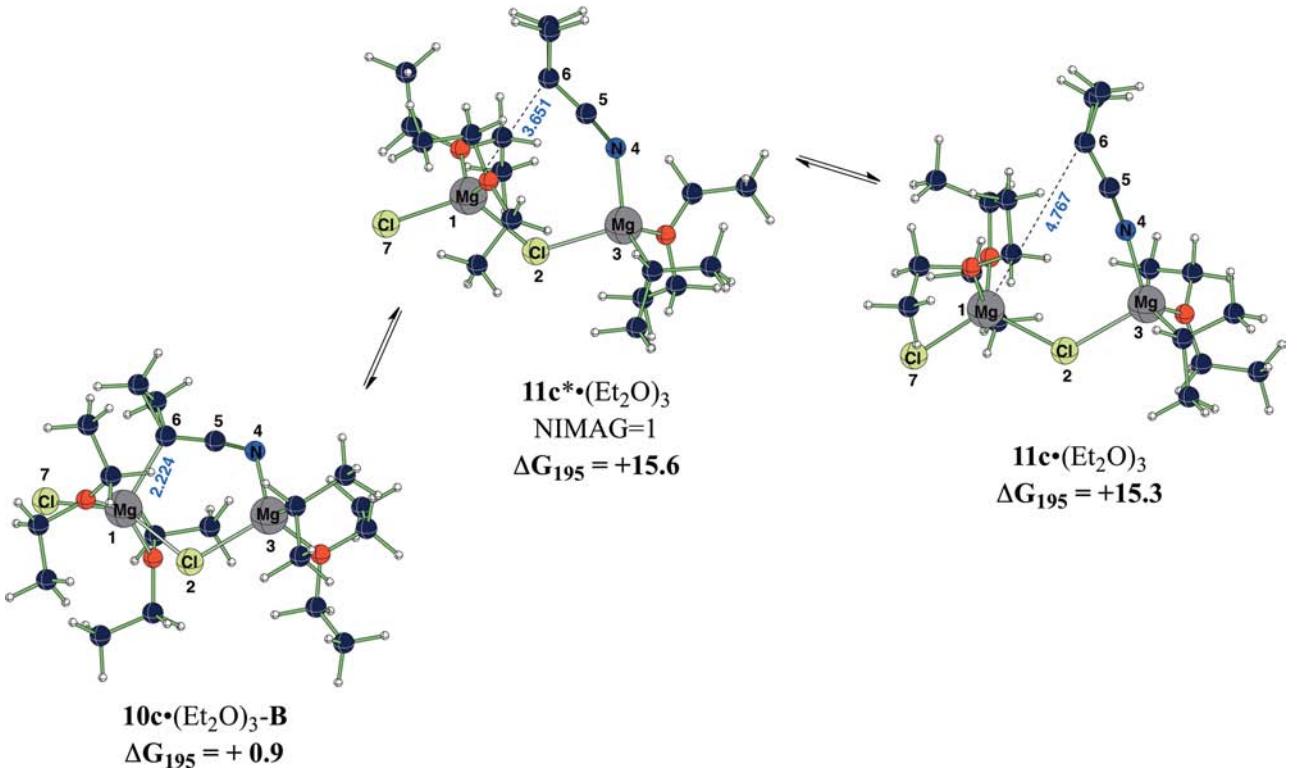

Figure 4. Possible reaction coordinates for ion-pair separation of trisolvated contact ion pair **10c**·$(Et_2O)_3$-**B**. Mg^1-C^6 distances (B3LYP/6-31G*) are given in angstroms, and values of ΔG_{195} (MP2/6-31G*(PCM)//B3LYP/6-31G*) are given in kilocalories per mole; *anti*-**10c**·$(Et_2O)_2$ (not shown) is the lowest energy species, at 0.0 kcal/mol.

related ion pair **11c**·$(Et_2O)_3$. The structures, Mg^1-C^6 distances, and relative free energies of these species are shown in Figure 4. Rupture of the Mg^1-C^6 bond in transition structure **11c***·$(Et_2O)_3$ is indicated by the motion associated with the sole imaginary frequency of this species and is consistent with the large increase in Mg^1-C^6 distances from **10c**·$(Et_2O)_3$-**B** to **11c***·$(Et_2O)_3$ to **11c**·$(Et_2O)_3$ (>2.5 Å, Figure 4). Concurrent with this change are significant *decreases* in the Mg^1-Cl^2 (−0.3 Å) and Mg^1-O (−0.1 Å) bond lengths (see the Supporting Information for additional bond length information). The shortening of these bonds should effect stabilization of the formal cation on Mg^1 in the separated ion pair **11c**·$(Et_2O)_3$. We would stress that we have not made an exhaustive search for other transition structures that might be relevant to stereochemical inversion of **7a** or of *trans*-**7b**. Nevertheless, the relative free energy of **11c***·$(Et_2O)_3$ at MP2/6-31G*(PCM)//B3LYP/6-31G* is 15.6 kcal/mol, which is serendipitously very close to the aforementioned experimental values of $\Delta G^{\ddagger}_{enant}$ for **1a** and $\Delta G^{\ddagger}_{epi}$ for *trans*-**1b** in pure Et_2O at 195 K (15.4 ± 0.1 and 15.5 ± 0.1 kcal/mol, respectively). This close correspondence therefore suggests that such a transition structure could correspond to the rate-determining step of stereochemical inversion of **1a** and *trans*-**1b**. Note that **11c***·$(Et_2O)_3$ represents a dissociative ion-pair separation transition structure; we have previously characterized an associative tetrakis(THF)-solvated transition structure for ion-pair separation of the tris(THF) solvate of trityllithium.[42] Finally, the related separated ion pair **11c**·$(Et_2O)_3$ is only slightly lower in energy than the ion-pair separation transition structure and features a highly pyramidalized cyclopropylnitrile anion, η^1-bound to a four-coordinate Mg via the nitrile N atom. On the basis of these calculations, a possible mechanism of epimerization can now be envisioned with greater structural detail (Scheme 6).

We propose the rate-determining step of epimerization of the Grignard heterodimer is dissociation of the Mg^1-C^6 bond in *trans*-**10b**·$(Et_2O)_3$, which generates the separated ion pair *trans*-**11b**·$(Et_2O)_3$. Pyramidal inversion to give *cis*-**11b**·$(Et_2O)_3$ should be fast, based on the low activation energy calculated for cyclopropylnitrile carbanion itself (9.0 kcal/mol at MP2/6-31+G*).[47] Finally, rotation around the Mg−N bond and collapse of the ion pair should rapidly give *cis*-**10b**·$(Et_2O)_3$. Since the cyclopropylnitrile moiety remains bound to a Mg atom throughout this process, we term this mechanism an "ionogenic conducted tour".

■ CONCLUSION

In view of the growing importance of enantioenriched Grignard reagents and metalated nitriles, we undertook studies of the stereochemical inversion of a chiral Grignard reagent formed by Mg/Br exchange of bromonitrile *trans*-**2b**. Studies of its epimerization rate constant k_{tc} revealed a great sensitivity to the identity and concentration of the ethereal solvent. At 195 K, compared to reaction in 0.12 M Et_2O in toluene, the Grignard reagent derived from *trans*-**2b** epimerized 26-, 800-, and 1,300-fold faster in pure Et_2O, 2-MeTHF, and THF. Others have noted that, in reactions of enantioenriched stabilized organolithiums, use of Et_2O in place of THF can afford superior results. Takeda and co-workers demonstrated improved enantiomeric excess in Et_2O for epoxysilane rearrangement of α-cyanocarbanions[48] and Wittig rearrangement of benzylic carbanions.[49,50] Gawley and co-workers also observed that racemization rates of a lithiated Boc-pyrrolidine increased in the series Et_2O < 2-MeTHF < THF.[6] These trends are likely due in

dx.doi.org/10.1021/ja407348s | J. Am. Chem. Soc. 2013, 135, 14390−14400

Scheme 6. Proposed Epimerization Mechanism Following Mg/Br Exchange of *trans*-2b

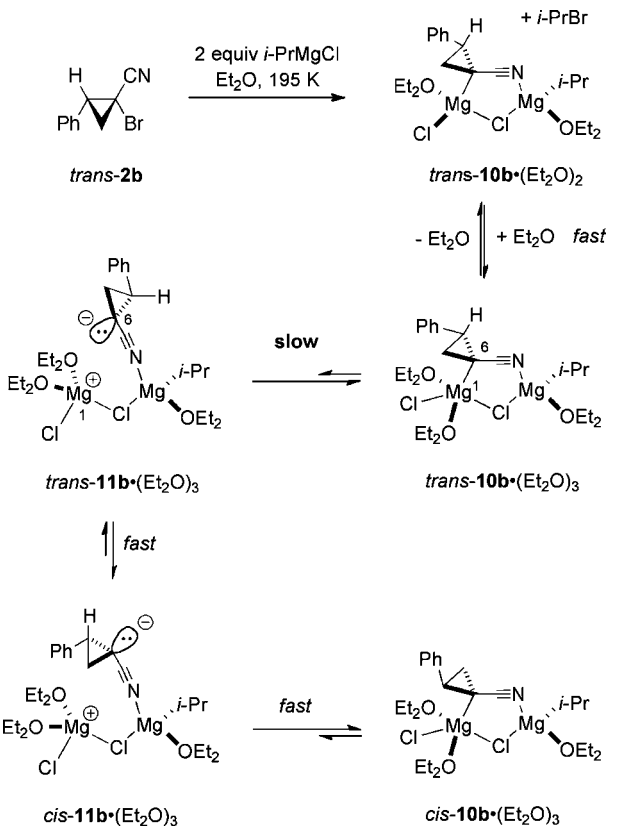

part to increasing solvating power along this series of ethers, as Collum demonstrated in studies of solvation of LiHMDS[51] and LDA,[52] but the present study provides a useful and compelling demonstration of the possible magnitude of this effect and illustrates that, even in the case of "superior" solvents such as Et_2O, addition of a hydrocarbon cosolvent can further improve configurational stability.[53]

Reaction stoichiometry studies of the Mg/Br exchange of *trans*-**2b** with *i*-PrMgCl suggests formation of a monomeric species (i.e., **1b**) in THF. However, in Et_2O, 2 equiv of *i*-PrMgCl is required for full conversion of *trans*-**2b**, as we had shown earlier for Mg/Br exchange of **2a**. This observation, combined with the known dimeric state of alkylmagnesium chlorides in Et_2O,[35−37] suggests that in this solvent Mg/Br exchange of *trans*-**2b** yields the heterodimer **7b**. Studies in toluene/Et_2O mixtures showed a saturating dependence of k_{tc} on [Et_2O] at 195, 212, and 231 K. This behavior was proposed to arise from rapid incremental solvation of a disolvate, followed by slow epimerization. Analysis of these rate constants allowed extrapolation of K_{solv}, the equilibrium constant for incremental solvation. The derived Gibbs free energies (ΔG_{solv}) indicated incremental solvation was nearly thermoneutral (−0.30 kcal/mol at 195 K to +0.17 kcal/mol at 231 K), and the associated entropy change ΔS_{solv} (−13 ± 3 eu) was consistent with capture of a solvent ligand. Eyring analysis of k_{tc} at five different concentrations of Et_2O consistently indicated negative entropies of activation for epimerization ($\Delta S^{\ddagger}_{epi}$ = −21 ± 13 to −34 ± 9 eu). Since the solvation number does not change in the rate-determining step of epimerization, these negative activation entropies appear most consistent with a reordering of the solvent shell. Such reordering (electrostriction[23]) would be expected to accompany the increase in dipole moment during ion-pair separation. Thus, the kinetics of epimerization of *trans*-**7b** mirrored the behavior we had seen earlier for enantiomerization of the related heterodimer **7a**,[21] while providing considerably more detail on the thermodynamics of incremental solvation.

Computational studies were then carried out on explicit Et_2O solvates of heterodimers of *i*-PrMgCl and (1-cyanocyclopropyl) magnesium chloride (**1c**) to determine possible structures for the intermediates involved in stereochemical inversion of *trans*-**7b** and **7a**. The most stable heterodimer was found to be a disolvate (*anti*-**10c**·$(Et_2O)_2$), which featured a bridging chloride and a bridging cyclopropylnitrile unit. At the MP2/6-31G*-(PCM)//B3LYP-6-31G* level three trisolvates were found to be within 2.0 kcal/mol of the low-energy structure, similar to our observation that incremental solvation was nearly thermoneutral. Finally, a transition structure for rupture of the Mg−C bond (**11c***·$(Et_2O)_3$) was located with a relative free energy (ΔG_{195} = 15.6 kcal/mol) that was serendipitously very close to the experimental activation free energy for epimerization of *trans*-**7b** in pure Et_2O at 195 K (15.5 ± 0.1 kcal/mol). This transition structure and a related separated ion pair both retain a N-bound cyclopropylnitrile unit, thus supporting an ionogenic conducted tour mechanism for stereochemical inversion of **7a** and **7b**.

EXPERIMENTAL SECTION AND COMPUTATIONAL METHODS

General Procedures. ^{1}H NMR spectra were recorded at 500 or 400 MHz; the corresponding ^{13}C NMR resonant frequencies were 126 and 101 MHz, respectively. Tetrahydrofuran (THF), 2-methyltetrahydrofuran (2-MeTHF), and diethyl ether (Et_2O) were distilled from sodium/benzophenone ketyl immediately prior to use in reactions. Toluene was distilled from CaH_2 immediately prior to use, and methylene chloride was dried by distillation from calcium hydride and storage over activated 4 Å molecular sieves. Grignard reagents were purchased as solutions in the desired solvent: *i*-PrMgCl (2.0 M in THF), *i*-PrMgCl (1.0 M in 2-MeTHF), and *i*-PrMgCl (1.0 M in Et_2O). The actual concentration of active Grignard reagent was determined using the standard *sec*-butanol/phenanthroline titration procedure.[34] Reactions at 195 K were maintained using the standard acetone/dry ice bath. Temperatures of 212 and 231 K were achieved using a Neslab Cryocool CC-100 immersion cooler. Reaction stoichiometry (Table 1) was assessed by monitoring two independent measures of reaction progress. First, conversion (%) of *trans*-**2b** to *trans*- and *cis*-d_1-**3b** was determined by ^{1}H NMR integrations. Second, the amount of *i*-PrBr formed was determined by GC−MS using mesitylene as an internal standard, as detailed in our recent paper.[21]

***cis*-1-Bromo-2-phenylcyclopropanecarboxamide (*cis*-5).** *n*-BuLi (2.5 M in hexane, 2.2 mL, 5.5 mmol) was added to a stirred solution of 2,2-dibromocyclopropylbenzene (**6**)[30] (1.38 g, 5 mmol) in THF (10 mL) at −78 °C under nitrogen and stirred for 30 min. CO_2 was bubbled into this solution via cannula from another flask containing chunks of dry ice (ca. 2.5 g), over the course of 3.5 h at −78 °C. The reaction was then quenched with water (10 mL) and diluted with Et_2O (50 mL). The phases were then separated, and the organic phase was washed with saturated $NaHCO_3$ solution (3 × 20 mL). The aqueous phases were combined and acidified with concd HCl and extracted with Et_2O (3 × 30 mL). The ether phases were combined, dried over sodium sulfate, filtered, and concentrated in vacuum to give the carboxylic acid intermediate as an off-white-colored solid,[31] which was used directly for the next step without purification. Thionyl chloride (7.3 mL, 100 mmol) was added, followed by DMF (0.5 mL). The resulting solution was stirred at room temperature overnight. The volatiles were removed in vacuo, the residue was dissolved in $CHCl_3$ (30 mL), and concd aq NH_4OH (37 mL) was

dx.doi.org/10.1021/ja407348s | J. Am. Chem. Soc. 2013, 135, 14390−14400

added dropwise at room temperature. After vigorous stirring overnight, volatiles were removed in vacuo, and $CHCl_3$ (50 mL) and water (50 mL) were added. The organic layer was separated, the aqueous layer was extracted with $CHCl_3$ (2 × 30 mL), and the combined organic extracts were washed with brine (20 mL), dried over Na_2SO_4, and concentrated in vacuo. The residue was purified by silica gel column chromatography (25% EtOAc in hexanes) to give *cis*-**5** (600 mg, 50% yield for two steps) as a white solid: mp 76−77 °C; ^{1}H NMR (500 MHz, $CDCl_3$) δ 7.32−7.20 (m, 5H), 6.23 (s, 1H), 5.83 (s, 1H), 3.02 (dd, J = 8.8, 10.0 Hz, 1H), 2.41 (dd, J = 6.6, 8.8 Hz, 1H), 1.71 (dd, J = 6.6, 10.0 Hz, 1H); ^{13}C NMR (126 MHz, $CDCl_3$) δ 168.1, 134.4, 128.9, 128.3, 127.4, 37.0, 34.3, 21.3; HRMS (ESI+) m/z calcd for $C_{10}H_{11}{}^{79}BrNO$ [M + H] 240.0024, found 240.0009; calcd for $C_{10}H_{11}{}^{81}BrNO$ [M + H] 242.0004, found 241.9989.

***cis*-1-Bromo-2-phenylcyclopropanecarbonitrile (*cis*-2b).** Amide *cis*-**5** (989 mg, 4.1 mmol) and *p*-TsCl (2.5 g, 13.0 mmol) were combined in pyridine (40 mL) and stirred at 80 °C for 1 day. A 100 mL volume of aqueous HCl (6 M) solution was added, and the resulting aqueous solution was extracted with ethyl acetate (3 × 30 mL). The combined organic solution was washed with brine, dried over Na_2SO_4, and concentrated in vacuo. The residue was purified by silica gel column chromatography (4% EtOAc in hexanes) to give *cis*-**2b** (805 mg, 88%) as a colorless oil: ^{1}H NMR (500 MHz, $CDCl_3$) δ 7.43−7.26 (m, 5H), 2.99 (dd, J = 8.1, 9.9 Hz, 1H), 2.17 (dd, J = 7.3, 8.1 Hz, 1H), 1.95 (dd, J = 7.3, 9.9 Hz, 1H); ^{13}C NMR (126 MHz, $CDCl_3$) δ 133.2, 129.0, 128.6, 128.0, 117.3, 35.3, 24.0, 11.6. Anal. Calcd for $C_{10}H_8BrN$: C, 54.08; H, 3.63; N, 6.31. Found: C, 54.35; H, 3.71; N, 6.26.

***trans*-1-Bromo-2-phenylcyclopropanecarboxamide (*trans*-5).** To a solution of *trans*-**4**[29] (3.2 g) in THF (105 mL) was added a solution of $LiOH{\cdot}H_2O$ (7.6 g) in water (105 mL) at 0 °C. The resulting solution was stirred at room temperature overnight. The THF was removed in vacuo, and the remaining aqueous solution was acidified with 3 M HCl with stirring until a large amount of white precipitate appeared. The white solid was filtered and washed with hexanes to give the corresponding carboxylic acid. This material (1.2 g, 5 mmol) was dissolved in thionyl chloride (7.3 mL, 100 mmol), and DMF (0.5 mL) was added. After the solution was stirred overnight at room temperature, the volatiles were removed in vacuo and the residue was dissolved in 30 mL of $CHCl_3$. Concentrated NH_4OH (37 mL) was added dropwise at room temperature, after which the reaction mixture was stirred vigorously overnight. Volatiles were removed in vacuo, and $CHCl_3$ (50 mL) and water (50 mL) were added into the reaction mixture. The organic layer was separated, and the aqueous layer was extracted with $CHCl_3$ (2 × 30 mL). The combined organic fractions were washed with brine (20 mL), dried over Na_2SO_4, and concentrated in vacuo. The residue was purified by silicon gel column chromatography (25% EtOAc in hexanes) to give *trans*-**5** (980 mg, 82%) as a white solid: mp 117−118 °C; ^{1}H NMR (400 MHz, $CDCl_3$) δ 7.38−7.21 (m, 5H), 6.81 (s, 1H), 6.35 (s, 1H), 3.07−2.95 (m, 1H), 2.23 (dd, J = 6.0, 10.2 Hz, 1H), 1.75 (dd, J = 6.0, 8.5 Hz, 1H); ^{13}C NMR (101 MHz, $CDCl_3$) δ 171.7, 136.2, 129.3, 128.2, 127.5, 38.6, 32.5, 23.1; HRMS (ESI+) m/z calcd for $C_{10}H_{11}{}^{79}BrNO$ [M + H] 240.0024, found 240.0000; calcd for $C_{10}H_{11}{}^{81}BrNO$ [M + H] 242.0004, found 241.9980.

***trans*-1-Bromo-2-phenylcyclopropanecarbonitrile (*trans*-2b).** *trans*-**5** (900 mg, 3.8 mmol) was dehydrated with the same procedure given for *cis*-**2b** to afford *trans*-**2b** (724 mg, 87%) as a white solid: mp 53−54 °C; ^{1}H NMR (500 MHz, $CDCl_3$) δ 7.41−7.35 (m, 3H), 7.25−7.21 (m, 2H), 2.95 (dd, J = 8.7, 10.2 Hz, 1H), 2.21 (dd, J = 7.1, 10.2 Hz, 1H), 1.86 (dd, J = 7.1, 8.7 Hz, 1H); ^{13}C NMR (126 MHz, $CDCl_3$) δ 133.3, 129.4, 128.6, 128.5, 119.9, 31.9, 22.4, 14.4. Anal. Calcd for $C_{10}H_8BrN$: C, 54.08; H, 3.63; N, 6.31. Found: C, 54.26; H, 3.67; N, 6.30.

***cis*- and *trans*-2-Phenylcyclopropanecarbonitrile (*cis*-3b and *trans*-3b).** These compounds were prepared according to the method of Kaiser et al.[54] from trimethylsulfoxonium iodide (1.1 g, 5 mmol) and cinnamonitrile (516.6 mg, 4 mmol). After aqueous workup the residue was purified by silica gel column chromatography (2−5%, EtOAc in hexanes) to give *cis*-**3b** (oil, 97 mg, 17%) and *trans*-**3b** (white solid, 218 mg, 38%, mp 51.6 −53.2 °C). These compounds were consistent with ^{1}H NMR data in the literature,[55] but we provide a more detailed tabulation below.

Data for *cis*-**3b**: ^{1}H NMR (500 MHz, $CDCl_3$) δ 7.40−7.26 (m, 5H), 2.53 (ddd, J = 7.5, 8.5, 8.5 Hz, 1H), 1.83 (ddd, J = 6.0, 8.5, 9.0 Hz, 1H), 1.59−1.55 (m, 2H); ^{13}C NMR (126 MHz, $CDCl_3$): δ 135.2, 128.6, 128.0, 127.7, 119.4, 23.2, 12.9, 6.4; HRMS (ESI) m/z calcd for $C_{10}H_{10}N$ [M + H] 144.0735, found 144.0808.

Data for *trans*-**3b**: ^{1}H NMR (500 MHz, $CDCl_3$) δ 7.35−7.11 (m, 5H), 2.63 (ddd, J = 5.0, 7.0, 9.5 Hz, 1H), 1.62 (ddd, J = 5.5, 5.5, 9.5 Hz, 1H), 1.55 (ddd, J = 5.0, 5.5, 9.0 Hz, 1H), 1.45 (ddd, J = 5.5, 7.0, 9.0 Hz, 1H); ^{13}C NMR (126 MHz, $CDCl_3$) δ 137.6, 128.8, 127.4, 126.4, 121.1, 24.9, 15.3, 6.7; HRMS (ESI) m/z calcd for $C_{10}H_{10}N$ [M + H] 144.0735, found 144.0808.

General Procedure for Mg/Br Exchange/$DOCH_3$ Trapping Experiments. Four flame-dried 10 mL long-neck round-bottom flasks (custom built, necks 7.5 cm long) were each charged with bromonitrile **2b** (*trans* or *cis*,12.5 mg, 0.0563 mmol) and a magnetic stirbar, capped with rubber septa, and purged with nitrogen. Freshly distilled solvent (1.0 mL) was then added, and the flasks were all placed in the same constant-temperature bath set at the required temperature using the appropriate cooling method (described above). After these reaction flasks were allowed to cool to the correct temperature for 15 min, *i*-PrMgCl (2.2 equiv, 0.124 mL of 1.0 M commercial solution, precooled for 15 min in a separate flask in the same dewar) was added. At this point $[Mg]_{total}$ = 0.110 M and $[\mathbf{2b}]_0$ = 0.05 M. Following the desired delay time t, the reactions were quenched by a quick addition of CH_3OD (99.98% D, 0.1 mL) from a flask that had been precooled to the reaction temperature for 15 min using a syringe that had also been precooled by flushing several times with cold CH_3OD. After removal of each flask from the cooling bath, solvent was removed in vacuo. The residue was dissolved in $CDCl_3$, filtered to remove Mg salts, and analyzed by ^{1}H NMR spectroscopy. In each case >99% conversion of starting material and >95% deuterium incorporation in **3b** were observed, allowing easy measurement of the dr value of d_1-**3b**.

***cis*-1-Deuterio-2-phenylcyclopropanecarbonitrile (*cis*-d_1-3b).** This compound was prepared from *cis*-**2b** (50 mg, 0.23 mmol) using the procedure above, −78 °C, using a 1 min delay time and a CH_3OD quench. The product was obtained in quantitative yield as an oil (32 mg), and the observed dr was <2:98: ^{1}H NMR (500 MHz, $CDCl_3$) δ 7.40−7.33 (m, 2H), 7.32−7.26 (m, 4H), 2.53 (t, J = 7.9 Hz, 1H), 1.60−1.47 (m, 2H); ^{13}C NMR (126 MHz, $CDCl_3$) δ 135.2, 128.6, 128.0, 127.6, 119.4, 23.1, 12.8, 6.2 (1:1:1 triplet, $^1J_{C-D}$ = 26.7 Hz); HRMS (ESI) m/z calcd for $C_{10}H_9DN$ [M + H] 145.0798, found 145.0859.

***trans*-1-Deuterio-2-phenylcyclopropanecarbonitrile (*trans*-d_1-3b).** This compound was prepared from *trans*-**2b** (50 mg, 0.23 mmol) using the procedure above, −78 °C, using a 1 min delay time and a CH_3OD quench. The product was obtained in quantitative yield as a white solid (31 mg, 98% yield, mp 51.1−52.8 °C), and the observed dr was >98:2: ^{1}H NMR (500 MHz, $CDCl_3$) δ 7.35−7.23 (m, 3H), 7.13−7.07 (m, 2H), 2.62 (dd, J = 9.2, 6.8 Hz, 1H), 1.71−1.52 (m, 1H), 1.44 (t, J = 6.7, 5.5, 1.2 Hz, 1H); ^{13}C NMR (126 MHz, $CDCl_3$) δ 137.6, 128.8, 127.4, 126.3, 121.0, 24.8, 15.1, 6.4 (1:1:1 triplet, $^1J_{C-D}$ = 26.8 Hz); HRMS (ESI) m/z calcd for $C_{10}H_9DN$ [M + H] 145.0798, found 145.0866.

Mg/Br Exchange/$DOCH_3$ Trapping Experiments at Varying $[Mg]_{total}$ in Et_2O. Reactions at $[Mg]_{total}$ of 0.025 and 0.125 M were performed in Et_2O similarly to the general procedure above. Reactions at $[Mg]_{total}$ = 0.006 and 0.0125 M were performed in 50 and 25 mL round-bottom flasks, respectively. In both of these cases, 0.1 mL or 100 equiv of CH_3OD was added to ensure rapid and complete quench of the organomagnesium species in these solutions of significantly larger volume.

Mg/Br Exchange/$DOCH_3$ Trapping Experiments at Varying [Et_2O]. Four flame-dried 10 mL long-neck round-bottom flasks (custom built necks 7.5 cm long) were each charged with bromonitrile *trans*-**2b** (12.6 mg, 0.0567 mmol) and a magnetic stirbar, capped with rubber septa, and purged with nitrogen. Freshly distilled Et_2O (1.5 mL) and toluene (8 mL) were added (total volume 9.5 mL) to achieve

the intended final concentration of Et_2O in toluene after addition of the Grignard reagent (see below), and the flasks were all placed in the same constant-temperature bath set at the required temperature using the appropriate cooling method (described above). After these reaction flasks were allowed to cool to the correct temperature for 15 min, *i*-PrMgCl (0.5 mL, 0.25 M in Et_2O, 2.2 equiv, solution precooled in the same bath) was added to these flasks via syringe. At this point the total volume was 10 mL, $[Mg]_{total}$ = 0.013 M, and $[Et_2O]$ ranged from 9.5 to 0.12 M, depending on the volumes of Et_2O and toluene added. Following delay times *t* of 1, 5, 10, and 20 min, the reactions were quenched, worked up, and analyzed as explained in the general procedure above.

Computational Methods. Calculations were performed using Gaussian 09.[56] Geometry optimization was performed at B3LYP/6-31G* for computational economy; this and similar method/basis set combinations have been used in other studies of Grignard reagents.[37,57,58] All stationary points were characterized by vibrational frequency analysis as minima (NIMAG = 0) or transition structures (NIMAG = 1). An exhaustive search of the conformational space of the coordinated Et_2O ligands was not undertaken. However, for each optimized structure, the coordinated Et_2O ligands were inspected to ensure no unnecessary steric clashes or *syn*-pentane-like conformations were present. PCM single-point calculations were performed with the options solvent = diethyl ether, surface = SES, and radii = Pauling; Pauling radii have been recommended for ionic species.[59] Relative free energies were calculated as described above; additional details are provided in the Supporting Information.

■ ASSOCIATED CONTENT

Supporting Information

NMR spectra for all synthesized compounds, derivation of eq 1 and the equation in Scheme 5, error analysis method, raw dr data for kinetic plots, electronic energies, thermodynamic corrections, selected bond lengths, and Cartesian coordinates of all calculated species. This material is available free of charge via the Internet at http://pubs.acs.org.

■ AUTHOR INFORMATION

Corresponding Author

pcarlier@vt.edu

Notes

The authors declare no competing financial interest.

■ ACKNOWLEDGMENTS

We gratefully acknowledge support from the National Science Foundation (Grant CHE-075006).

■ REFERENCES

(1) Basu, A.; Thayumanavan, S. *Angew. Chem., Int. Ed.* **2002**, *41*, 716−738.

(2) Clayden, J. *Organolithiums: Selectivity for Synthesis*; Pergamon: Amsterdam, 2002, pp 169−240.

(3) Capriati, V.; Florio, S.; Salomone, A. In *Stereochemical Aspects of Organolithium Compounds*; Gawley, R. E., Ed.; Verlag Helvetica Chimica Acta and Wiley-VCH: Zürich, Switzerland, 2010; Vol. *26*, p 135−164.

(4) Gawley, R. E. In *Stereochemical Aspects of Organolithium Compounds*; Gawley, R. E., Ed.; Verlag Helvetica Chimica Acta and Wiley-VCH: Zürich, Switzerland, 2010; Vol. *26*, pp 93−133.

(5) Mitchell, E. A.; Peschiulli, A.; Lefevre, N.; Meerpoel, L.; Maes, B. U. W. *Chem.—Eur. J.* **2012**, *18*, 10092−10142.

(6) Beng, T. K.; Woo, J. S.; Gawley, R. E. *J. Am. Chem. Soc.* **2012**, *134*, 14764−14771.

(7) Tait, M.; Donnard, M.; Minassi, A.; Lefranc, J.; Bechi, B.; Carbone, G.; O'Brien, P.; Clayden, J. *Org. Lett.* **2013**, *15*, 34−37.

(8) Hoffmann, R. W.; Nell, P. G. *Angew. Chem., Int. Ed.* **1999**, *38*, 338−340.

(9) Hoffmann, R. W.; Hölzer, B.; Knopff, O.; Harms, K. *Angew. Chem., Int. Ed.* **2000**, *39*, 3072−3074.

(10) Hoffmann, R. W. *Chem. Soc. Rev.* **2003**, *32*, 225−230.

(11) Satoh, T.; Fukuda, Y. *Tetrahedron* **2003**, *59*, 9803−9810.

(12) Mitsunaga, S.; Ohbayashi, T.; Sugiyama, S.; Saitou, T.; Tadokoro, M.; Satoh, T. *Tetrahedron: Asymmetry* **2009**, *20*, 1697−1708.

(13) Barsamian, A. L.; Blakemore, P. R. *Organometallics* **2012**, *31*, 19−22.

(14) Rayner, P. J.; O'Brien, P.; Horan, R. A. J. *J. Am. Chem. Soc.* **2013**, *135*, 8071−8077.

(15) Barker, G.; Alshawish, M. R.; Skilbeck, M. C.; Coldham, I. *Angew. Chem., Int. Ed.* **2013**, *52*, 7700−7703.

(16) Walborsky, H. M.; Young, A. E. *J. Am. Chem. Soc.* **1964**, *86*, 3288−3296.

(17) Fleming, F. F.; Zhang, Z.; Knochel, P. *Org. Lett.* **2004**, *6*, 501−503.

(18) Fleming, F. F.; Zhang, Z.; Liu, W.; Knochel, P. *J. Org. Chem.* **2005**, *70*, 2200−2205.

(19) Carlier, P. R.; Zhang, Y. *Org. Lett.* **2007**, *9*, 1319−1322.

(20) As an electrophilic quenching method, we view deuteration as superior to protonation. Immediately following Mg/Br exchange, it is conceivable that the newly formed Grignard reagent could cause elimination of *i*-PrBr, forming protio material (i.e., **3b**), before significant stereochemical inversion could occur. The use of a deuterium quench (precooled to the reaction temperature) after an equilibration time *t* therefore allows the extent of elimination to be assessed by ^{1}H NMR spectroscopy. Since in our reactions less than 2% protio material was seen, we can be confident that the measured er (or dr) ratios correspond closely to the stereochemical composition of the Grignard reagent at time *t*.

(21) Patwardhan, N. N.; Gao, M.; Carlier, P. R. *Chem.—Eur. J.* **2011**, *17*, 12250−12253.

(22) Eyring, H. *Chem. Rev.* **1935**, *17*, 65−77.

(23) Ahlbrecht, H.; Harbach, J.; Hoffmann, R. W.; Ruhland, T. *Liebigs Ann. Chem.* **1995**, 211−216.

(24) Hoell, D.; Schnieders, C.; Müllen, K. *Angew. Chem. Suppl.* **1983**, 299−306.

(25) Capriati, V.; Florio, S.; Perna, F. M.; Salomone, A. *Chem.—Eur. J.* **2010**, *16*, 9778−9788.

(26) Sasaki, M.; Takegawa, T.; Ikemoto, H.; Kawahata, M.; Yamaguchi, K.; Takeda, K. *Chem. Commun.* **2012**, *48*, 2897−2899.

(27) Nath, D.; Fleming, F. F. *Angew. Chem., Int. Ed.* **2011**, *50*, 11790−11793.

(28) Nath, D.; Fleming, F. F. *Chem.—Eur. J.* **2013**, *19*, 2023−2029.

(29) Bonge, H. T.; Pintea, B.; Hansen, T. *Org. Biomol. Chem.* **2008**, *6*, 3670−3672.

(30) Clayden, J.; Watson, D. W.; Chambers, M. *Tetrahedron* **2005**, *61*, 3195−3203.

(31) Nishii, Y.; Nagano, T.; Gotoh, H.; Nagase, R.; Motoyoshiya, J.; Aoyama, H.; Tanabe, Y. *Org. Lett.* **2007**, *9*, 563−566.

(32) Andraos, J. *J. Chem. Educ.* **1996**, *73*, 150−154.

(33) Connors, K. A. In *Chemical Kinetics: The Study of Reactions in Solution*; VCH: New York, 1990; pp 60−61.

(34) Watson, S. C.; Eastham, J. F. *J. Organomet. Chem.* **1967**, *9*, 165−168.

(35) Walker, F. W.; Ashby, E. C. *J. Am. Chem. Soc.* **1969**, *91*, 3845−3850.

(36) Seyferth, D. *Organometallics* **2009**, *28*, 1598−1605.

(37) Tammiku-Taul, J.; Burk, P.; Tuulmets, A. *J. Phys. Chem. A* **2004**, *108*, 133−139.

(38) Dohmeier, C.; Loos, D.; Robl, C.; Schnöckel, H.; Fenske, D. *J. Organomet. Chem.* **1993**, *448*, 5−8.

(39) Hibbs, D. E.; Jones, C.; Richards, F. A. *J. Chem. Soc., Dalton Trans.* **1999**, 3531−3532.

(40) Boche, G.; Marsch, M.; Harms, K. *Angew. Chem., Int. Ed. Engl.* **1986**, *25*, 373−374.

(41) Mori, T.; Kato, S. *J. Phys. Chem. A* **2009**, *113*, 6158−6165.

(42) Deora, N.; Carlier, P. R. *J. Org. Chem.* **2010**, *75*, 1061−1069.

(43) Dixon, D. D.; Tius, M. A.; Pratt, L. M. *J. Org. Chem.* **2009**, *74*, 5881−5886.
(44) Hoepker, A. C.; Collum, D. B. *J. Org. Chem.* **2011**, *76*, 7985−7993.
(45) Pratt, L. M.; Truhlar, D. G.; Cramer, C. J.; Kass, S. R.; Thompson, J. D.; Xidos, J. D. *J. Org. Chem.* **2007**, *72*, 2962−2966.
(46) Anslyn, E. V.; Dougherty, D. A. *Modern Physical Organic Chemistry*; University Science Books: Sausalito, CA, 2006; pp 208−212.
(47) Carlier, P. R. *Chirality* **2003**, *15*, 340−347.
(48) Sasaki, M.; Kawanishi, E.; Shirakawa, Y.; Kawahata, M.; Masu, H.; Yamaguchi, K.; Takeda, K. *Eur. J. Org. Chem.* **2008**, *2008*, 3061−3064.
(49) Sasaki, M.; Ikemoto, H.; Kawahata, M.; Yamaguchi, K.; Takeda, K. *Chem.—Eur. J.* **2009**, *15*, 4663−4666.
(50) Ikemoto, H.; Sasaki, M.; Takeda, K. *Eur. J. Org. Chem.* **2010**, 6642−6650.
(51) Lucht, B. L.; Collum, D. B. *J. Am. Chem. Soc.* **1995**, *117*, 9863−9874.
(52) Remenar, J. F.; Lucht, B. L.; Collum, D. B. *J. Am. Chem. Soc.* **1997**, *119*, 5567−5572.
(53) Collum has amply demonstrated other useful features of donor solvent/hydrocarbon mixtures. For example, addition of hydrocarbon cosolvents to reduce the ethereal solvent concentration can dramatically increase the rates of LDA-mediated reactions: Collum, D. B.; McNeil, A. J.; Ramirez, A. *Angew. Chem., Int. Ed.* **2007**, *46*, 3002−3017.
(54) Kaiser, C.; Trost, B. M.; Beeson, J.; Weinstock, J. *J. Org. Chem.* **1965**, *30*, 3972−3975.
(55) Wang, M.-X.; Feng, G.-Q. *New J. Chem.* **2002**, *26*, 1575−1583.
(56) Frisch, M. J.; Trucks, G. W.; Schlegel, H. B.; Scuseria, G. E.; Robb, M. A.; Cheeseman, J. R.; Scalmani, G.; Barone, V.; Mennucci, B.; Petersson, G. A.; Nakatsuji, H.; Caricato, M.; Li, X.; Hratchian, H. P.; Izmaylov, A. F.; Bloino, J.; Zheng, G.; Sonnenberg, J. L.; Hada, M.; Ehara, M.; Toyota, K.; Fukuda, R.; Hasegawa, J.; Ishida, M.; Nakajima, T.; Honda, Y.; Kitao, O.; Nakai, H.; Vreven, T.; Montgomery, J. A., Jr.; Peralta, J. E.; Ogliaro, F.; Bearpark, M.; Heyd, J. J.; Brothers, E.; Kudin, K. N.; Staroverov, V. N.; Kobayashi, R.; Normand, J.; Raghavachari, K.; Rendell, A.; Burant, J. C.; Iyengar, S. S.; Tomasi, J.; Cossi, M.; Rega, N.; Millam, J. M.; Klene, M.; Knox, J. E.; Cross, J. B.; Bakken, V.; Adamo, C.; Jaramillo, J.; Gomperts, R.; Stratmann, R. E.; Yazyev, O.; Austin, A. J.; Cammi, R.; Pomelli, C.; Ochterski, J. W.; Martin, R. L.; Morokuma, K.; Zakrzewski, V. G.; Voth, G. A.; Salvador, P.; Dannenberg, J. J.; Dapprich, S.; Daniels, A. D.; Farkas, Ö.; Foresman, J. B.; Ortiz, J. V.; Cioslowski, J.; Fox, D. J. *Gaussian 09*, revision A.02; Gaussian, Inc.: Wallingford, CT, 2009.
(57) Yamazaki, S.; Yamabe, S. *J. Org. Chem.* **2002**, *67*, 9346−9353.
(58) Jiménez-Osés, G.; Brockway, A. J.; Shaw, J. T.; Houk, K. N. *J. Am. Chem. Soc.* **2013**, *135*, 6633−6642.
(59) De Sterck, B.; Van Speybroeck, V.; Mangelinckx, S.; Verniest, G.; De Kimpe, N.; Waroquier, M. *J. Phys. Chem. A* **2009**, *113*, 6375−6380.